



Sexual dimorphism in shape and size of the neurocranium

Diana H. Toneva¹ · Silviya Y. Nikolova¹ · Elena D. Tasheva-Terzieva² · Dora K. Zlatareva³ · Nikolai E. Lazarov⁴

Received: 11 May 2022 / Accepted: 4 August 2022 / Published online: 9 August 2022

© The Author(s), under exclusive licence to Springer-Verlag GmbH Germany, part of Springer Nature 2022

Abstract

Sex identification is a primary step in forensic analysis of skeletal remains. The accuracy of sex estimation methods greatly depends on the sexual dimorphism manifested by the target anatomical region. The study aims to evaluate the sexual dimorphism in shape and size of the neurocranium and to compare the potential of shape and size of different cranial regions to classify correctly the male and female crania. The study was carried out on computed tomography images of 373 Bulgarian adults (161 males and 212 females). Three-dimensional coordinates of 32 landmarks were acquired. The landmarks were arranged in 4 configurations: neurocranium, frontal bone, parietotemporal region, and occipital bone. For each configuration, the presence of significant sex differences in shape and size was tested. Principal component analysis (PCA) was applied to explore the shape variation. The classification power of size and shape was tested using discriminant analysis and k-means clustering. The neurocranium shows significant sex differences in shape and size. The parietotemporal region is the most dimorphic neurocranial part in size and the frontal bone is the most differing one in shape. The size of the parietotemporal region and frontal bone classifies correctly more than 80% of the crania. The discrimination ability based on shape is rather low as the highest values of about 70% are obtained for the frontal and occipital bone. The PCA plots show large overlapping of the male and female crania. It can be inferred that the sex-specific size differences in the neurocranium are more important than the shape differences.

Keywords Neurocranium · Sexual dimorphism · Geometric morphometrics · 3D landmarks · Computed tomography

Introduction

The positive identification of unknown bone remains largely depends on the correct estimation of the biological profile. However, the accurate estimation of the components of the biological profile (sex, age, ancestry, stature) rests on the skeletal elements available for analysis and their state of preservation [1]. Sex estimation is a crucial point in the

identification process. Standards for sex estimation are developed for almost all bones and bone parts, and their accuracy varies due to the different manifestation of sexual dimorphism in the human skeleton [2]. It has now been considered that the successful sex identification depends not only on the anatomic regions of the skeleton but also on the selected method and the degree of sexual dimorphism exhibited by a given population [3].

Standard sexing methods are based on quantitative and qualitative traits. The methods changed over the years from visual inspection of the shape and size of the bones and separate anatomical structures to modern methods conducted in virtual environment and based on sophisticated calculations. The latter studies have included the use of machine learning algorithms on data obtained from digital images [4–8]. The development of current sexing methods in forensic field largely depends on the use of digital images. The three-dimensional (3D) images in particular enable a more detailed quantitative description of the anatomical structures. Furthermore, the usage of computer-based calculations derived from 3D models increases objectivity and

✉ Diana H. Toneva
ditoneva@abv.bg

¹ Department of Anthropology and Anatomy, Institute of Experimental Morphology, Pathology and Anthropology with Museum, Bulgarian Academy of Sciences, Acad. G. Bonchev Str., Bl. 25, 1113 Sofia, Bulgaria

² Department of Zoology and Anthropology, Faculty of Biology, Sofia University, 1164 Sofia, Bulgaria

³ Department of Diagnostic Imaging, Faculty of Medicine, Medical University of Sofia, 1431 Sofia, Bulgaria

⁴ Department of Anatomy, Histology and Embryology, Faculty of Medicine, Medical University of Sofia, 1431 Sofia, Bulgaria

repeatability compared to the traditional forensic techniques based on osteometric data [9]. Many recent studies have used computed tomography (CT) scans to investigate the sexual dimorphism in cranium and its bones [4, 5, 10–19]. In this regard, medical imaging modalities provide the possibility to study large samples of individuals from contemporary populations. Thus, the recent data collected from CT images are useful for improvement of classical methods for sex estimation and their adaptation to changing populations [20].

The study of cranial sexual dimorphism including the development of sex estimation models separately for neuro- and viscerocranium is applicable in forensic and bioarchaeological cases, where human skeletal remains are frequently incomplete or damaged [21]. The human neurocranium demonstrates sex differences in its morphology and has been widely used in the development of methods for sex estimation. The main function of the neurocranium is to protect the brain, meninges, cerebral vasculature, and other elements of the central nervous system. This part of the skull has undergone progressive evolutionary changes with noticeable increase in its dimensions as a result of changes in the skull development during the evolution of hominins [22]. At birth, the neurocranium is proportionally the largest part of the skull, since it has an essential part in early life in relation to brain growth, while the viscerocranium experiences a longer ontogenetic growth [2]. In this regard, the neurocranial complex finalizes growth earlier than the viscerocranium and its adult size is achieved by approximately 16 years of age [23]. The sex differences in the size of neurocranium start to appear from 9 to 11 years onwards, while the shape differences become evident later in the post-pubertal period of time [2].

Many morphoscopic traits of the neurocranium demonstrate sex differences and are involved in the sex estimation of unknown bone remains. The primary traits refer to the projection of glabellar region, the slope of the mid-sagittal contour of the frontal bone, the protrusion of the external occipital protuberance, the relative size of the mastoid process of temporal bone, etc. Besides, there is an extensive list of cranial measurements, which are included in a large number of discriminant models for sex estimation. However, the morphoscopic and morphometric approach based on one or several variables is quite limiting and incomplete. In this regard, digital morphometry based on the 3D coordinates of large number of landmarks provides a possibility for a more thorough investigation of the anatomical structures.

Data collected by landmark-based approach serve as a basis of geometric morphometric (GM) studies. GM is a set of analytical techniques introduced in the morphological field to enable more adequate definition, separation, and analysis of the size and shape components of a particular structure [24]. GM allows more effective capturing of the shape of anatomical structures and provides a proper

visualization of the differences and changes in cranial morphology [25]. Hence, the GM approach appears very appropriate to study sex differences. Sexual dimorphism in the neurocranium has been explored in a number of GM studies [3, 10, 26–30], but the obtained results have not been always consistent. Besides, the neurocranium has been rarely partitioned to study and compare the strength of the sex differences in its separate parts.

The aim of the present study is to evaluate the sex differences in the shape and size of the neurocranium using GM approach. Moreover, we compare the potential of the shape and size of different regions of the neurocranium to classify correctly the male and female crania. We also test if a reduction in the number of landmarks describing the neurocranium can provide satisfying classification results.

Material and methods

A total of 373 head CT scans of Bulgarian adults were used in the study. The CT scans were generated with a Toshiba *Aquilion 64* CT scanner under the following scanning protocol: 32×0.5 mm detector configuration, tube voltage of 120 kV, tube current ranging from 165 to 500 mA, and exposure time of 0.5 s. The images were reconstructed at the following parameters: a 512×512 reconstruction matrix, 0.5 mm slice thickness, 0.3 mm reconstruction interval, and the FC63 convolution kernel. The CT scanning was performed for diagnostic purposes during the period 2017–2021. Images showing any pathological lesions or abnormalities affecting the cranial bones were not included in the study. All DICOM series were used after anonymization of the personal information except for the data of sex and age. The study was approved by the Human Research Ethics Committee at the Institute of Experimental Morphology, Pathology and Anthropology with Museum, Bulgarian Academy of Sciences.

The sample consisted of 161 males (mean age: 55.4 ± 16.7 years; range: 19–86 years) and 212 females (mean age: 59.7 ± 16.2 years; range: 20–94 years). Based on the DICOM series, polygonal surface models (.stl format) of the skulls were created using InVesalius 3.1 (CTI, Brazil). The segmentation was based on the predefined threshold for bone tissue (227–3071 HU). Three-dimensional (3D) coordinates of 32 (10 mid-sagittal and 11 bilateral) landmarks describing the neurocranium were acquired (Table 1; Fig. 1). The landmarks were digitized using the “Pick Point” tool in MeshLab ver. 2016.12. [31]. The landmark digitization was carried out by one examiner.

The landmarks were arranged in 4 configurations: neurocranium, frontal bone, parietotemporal region, and occipital bone. Data for size (centroid size, CS) and shape (Procrustes coordinates) were obtained for each configuration. The CS

Table 1 Cranial landmarks

Landmarks	Description	Landmark configurations
<i>Midsagittal landmarks</i>		
Nasion (n)	The intersection point of the frontonasal suture and the midsagittal plane	NC, FB
Glabella (g)	The most forward projecting point in the midline of the frontal bone at the level of the supraorbital ridges	NC, FB
Metopion (m)	The intersection point of the horizontal line connecting the frontal eminences and the midsagittal plane	NC, FB
Bregma (b)	The intersection point of the coronal and sagittal sutures	NC, FB, PT
Obelion (ob)	The intersection point of the sagittal suture and the line connecting the parietal foramina	NC, PT
Lambda (l)	The intersection point of the sagittal and lambdoid sutures	NC, PT, OB
Opisthocranium (op)	The most posterior point on the occipital bone in the midsagittal plane	NC, OB
Inion (in)	The point of intersection of the superior nuchal lines with the midsagittal plane	NC, OB
Basion (ba)	The midpoint of the anterior margin of <i>foramen magnum</i>	NC, OB
Opisthion (o)	The midpoint of the posterior margin of <i>foramen magnum</i>	NC, OB
<i>Bilateral landmarks</i>		
Frontomalare-temporale (fmt)	The most lateral point on the zygomaticofrontal suture	NC, FB
Frontomalare-orbitale (fmo)	The point of intersection of the lateral orbital margin with the zygomaticofrontal suture	NC, FB
Frontotemporale (ft)	The most medial point on the temporal ridge of the frontal bone	NC, FB
Maxillofrontale (mf)	The point of intersection of the medial orbital margin with the frontomaxillary suture	NC, FB
Supraorbitale (so)	The most superior point of the superior orbital margin	NC, FB
Stephanion (st)	The intersection point of the coronal suture and the temporal line	NC, FB, PT
Sphenion (sph)	The most anterior endpoint of the sphenoparietal suture	NC, FB, PT
Asterion (ast)	The point of intersection of the lambdoid, occipitomastoid, and parietomastoid sutures	NC, PT, OB
Eurion (eu)	The most lateral point on the lateral surface of the cranium	NC, PT
Mastoidale (ms)	The most inferior point on the mastoid process	NC, PT
Porion (po)	The uppermost point on the margin of the external auditory meatus	NC, PT

NC, neurocranium; FB, frontal bone; PT, parietotemporal region; OB, occipital bone

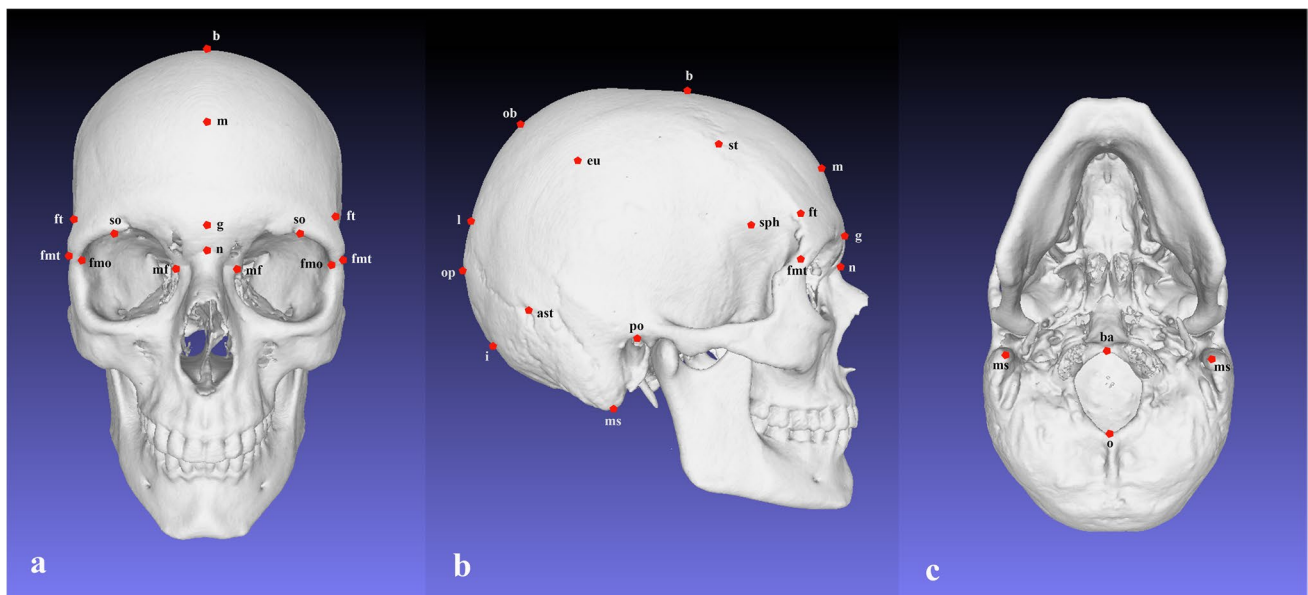


Fig. 1 Cranial landmarks: **a** frontal view; **b** lateral view; **c** inferior view

was computed as the square root of the sum of squared distances between the landmarks in a landmark set and their centroid and served as a measure of size of the corresponding landmark configuration of each specimen. The Procrustes coordinates were calculated using generalized Procrustes superimposition (GPS) of the raw coordinates of each dataset. These coordinates were generated after effectively removing the variation in position, size, and orientation from the raw landmark configurations. In addition, multivariate regression of the Procrustes coordinates (symmetric component) on ln-transformed CS was performed to correct the allometric effect of size on shape. The relationship between size and shape is an indication of the amount of shape changes per unit of size. Permutation test against the null hypothesis of independence between shape and size was applied with 10,000 randomization rounds. The regression residuals (size-corrected shape coordinates) were used for further analyses on shape of the studied configurations. The generalized Procrustes superimposition and multivariate regression were performed using MorphoJ, ver. 1.07a [32].

The significance of the sex differences in CS was evaluated by the Mann–Whitney *U*-test in SPSS (SPSS Inc, USA), because of failure of the normality and/or equal variance test. The sex differences in shape were tested for statistical significance by one-way PERMANOVA (in PAST, ver. 2.17c [33]), since a non-normal distribution was observed in all datasets. The multivariate normality of the shape variables was tested in advance by the Mardia's multivariate skewness and kurtosis tests using the online calculator at WebPower [34].

Principal component analysis (PCA) was applied to explore the shape variation of each configuration. For this purpose, variance–covariance matrices were generated using the regression residuals. The morphological variation associated with the extracted principal components (PCs) was visualized by wireframe graphs in MorphoJ. The wireframe graphs along the PC axes under observation were constructed at a scale factor of 0.1 Procrustes units.

Discriminant analysis (DA) was applied to assess the classification ability of each configuration to assign the crania to the correct sex. The DA was conducted on the following data describing the configurations: (1) CS; (2) PCs produced by PCA on the regression residuals and cumulatively accounting for 95% of the total variance; and (3) PCs produced by PCA on the combined data of shape variables and natural logarithm of CS and cumulatively accounting for 95% of the total variance. For all DA in our study, leave-one-out cross-validation procedure was used to calculate the classification accuracy. In addition, we applied k-means cluster analysis to the shape variables and combined size and shape data of each configuration. Unlike discriminant analysis, no prior information about the group affiliation of the specimens is required in k-means cluster analysis, so the clusters are

generated only based on the morphological similarity among the examples in each cluster. We set two clusters to group the crania and estimated the accuracy in relation to the actual sex of the individuals. The univariate and multivariate DA and the k-means cluster analysis were carried out in SPSS.

The classification accuracy was evaluated on an additional landmark configuration, which incorporated the landmarks demonstrating the greatest differences between the configurations of the male and female neurocrania. Thus, we aimed to compare the accuracy obtained on the full set of neurocranial landmarks with that achieved by the reduced set. That would allow us to establish if a smaller set of landmarks could provide similar accuracy to the full set.

The intraobserver error was evaluated based on 40 (20 male and 20 female) crania. The crania were digitized three times by one observer; each trial was performed on a separate day. Firstly, the intraobserver precision of digitization was evaluated for all landmarks based on their raw coordinates. For this purpose, the standard deviation of each landmark was calculated from the Euclidean distances obtained between the different placements of the landmark to its centroid. Thus, the measurement error of each landmark was estimated in millimeters based on its dispersion around the landmark centroid. In addition, the effect of the intraobserver error on size and shape of the neurocranium configuration was assessed by applying GPS and PCA to the sets of landmark coordinates from the three trials and by comparing the CS values and the ordination along the first two PCs. The CS values of the specimens were compared using technical error of measurement (TEM) and relative TEM. The scores of PC1 and PC2 were compared by intraclass correlation coefficient (ICC, Absolute Agreement). The ICC values were referred to poor (<0.50), moderate (0.50–0.75), good (0.75–0.90), or excellent reliability (>0.90) [35]. Besides, a scatterplot was used to visualize the clustering of the different trials for each specimen along the first two PCs. For evaluation of the interobserver error, thirty crania were digitized once by a second investigator and the obtained data were compared to those of the first investigator by applying the same procedures.

Results

Intra- and interobserver error

The intraobserver measurement errors of all landmarks were within 1.5 mm and most of them had values of less than 0.5 mm (Suppl. file 1). The values of the interobserver errors were larger than the intraobserver ones, but also almost all values were within 1.5 mm as only those for the right and left eurion were around and more than 2 mm. The values for the intraobserver TEM and rTEM obtained for the CS

were 0.45 mm and 0.10%, respectively. The corresponding values for the interobserver TEM and rTEM were 1.15 mm and 0.26%. The ICCs obtained for the PC1 and PC2 scores between the three trials of the principal investigator indicated excellent reliability (PC1: 0.986; PC2: 0.993). The results of the interobserver comparison showed excellent agreement for PC1 (0.928) and good agreement for the PC2 scores (0.884). The scatterplot illustrating the distribution of the three trials of the first investigator along the PC1 and PC2 axes showed that they clustered closely together for most of the 40 crania (Fig. 2), while the plotted data obtained from the two investigators were comparatively more dispersed (Suppl. file 2). Based on the obtained results, the precision error of the landmark digitization was assessed as acceptable.

Centroid size differences

The male neurocrania had significantly greater mean CS compared to the female ones. Significant sex differences

were also observed for the landmark configurations of the frontal bone, parietotemporal region, and occipital bone (Table 2).

Allometry

Multivariate regression of the Procrustes coordinates on CS was conducted for all configurations. For the neurocranium configuration, the size accounted for 3.2% of the total shape variation ($p < 0.0001$). The separate neurocranial regions also showed statistically significant dependence between shape and CS ($p < 0.0001$), but size explained a varying percentage of the total morphological variation (frontal bone: 3.1%; parietotemporal region: 1.6%; occipital bone: 5.7%). Because of the significant effect of size on shape established in all configurations, the residuals of the multivariate regressions were used for further analyses on shape.

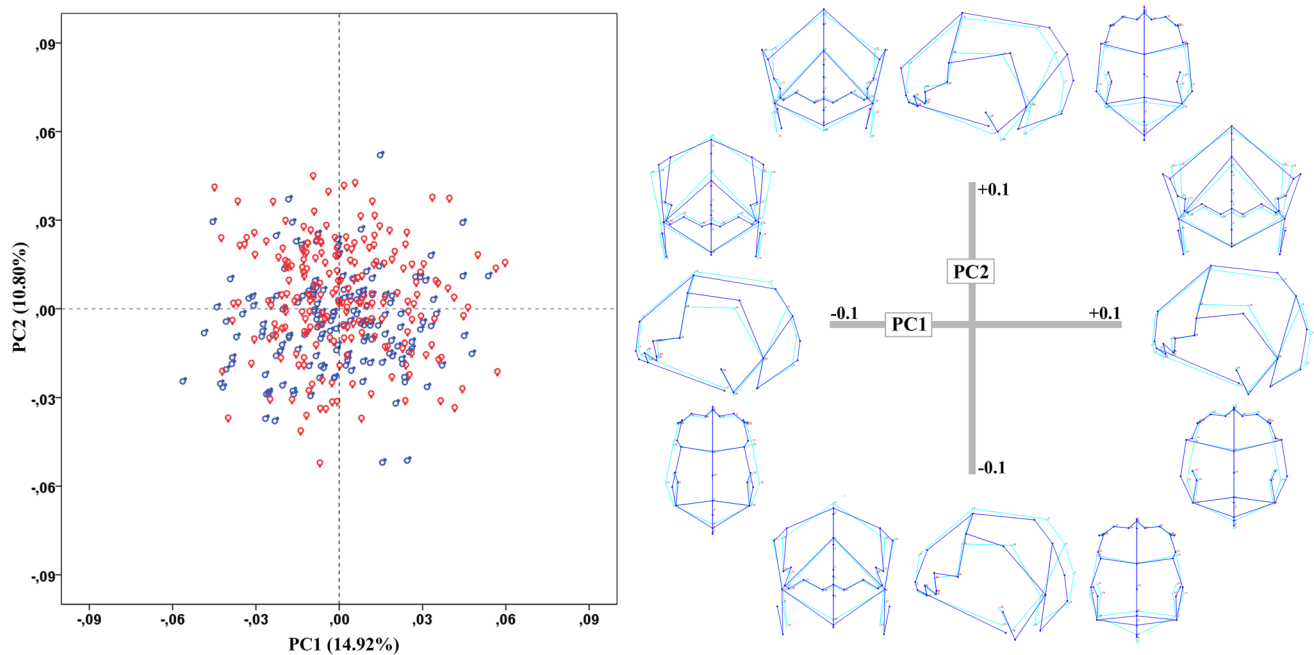


Fig. 2 Scatterplot of PC1 vs PC2 for the neurocranium. The wireframes illustrate the shape variation along the PC1 and PC2 axes. Blue male sign (♂) – male crania; red female sign (♀) – female crania

nia; light blue wireframe – the mean shape; dark blue wireframe – extreme shape configurations

Table 2 Centroid size of the landmark configurations in males and females

Landmark configuration	Males		Females		U-test
	Mean	SD	Mean	SD	
Neurocranium	461.98	13.53	438.58	10.46	$U=2417.00, p < 0.001$
Frontal bone	228.70	8.43	217.84	6.19	$U=4755.00, p < 0.001$
Parietotemporal region	311.12	10.04	296.43	7.64	$U=3796.00, p < 0.001$
Occipital bone	136.76	5.89	131.61	4.98	$U=8546.00, p < 0.001$

Shape differences

The shape of the neurocranium differed significantly between the male and female crania ($F=3.90$, $p=0.0001$). Significant sex differences were also observed in the shape of the frontal bone ($F=29.90$, $p=0.0001$), parietotemporal region ($F=8.15$, $p=0.0001$), and occipital bone ($F=11.69$, $p=0.0001$).

PCA on shape variables

The scatterplots of the first two PCs obtained after PCA on the regression residuals of all configurations are shown in Figs. 2, 3, 4, and 5. All scatterplots demonstrated considerable overlapping between the male and female crania. The results of PCA on the neurocranium configuration showed that the greatest shape variation in the sample was associated with the overall cranial shape which changed from an elongated and narrow neurocranium at the extreme negative values to a round shaped neurocranium at the extreme positive ones (Fig. 2). The shape variation along the PC1 axis of the frontal bone configuration indicated shape changes in the relative width and convexity of the frontal bone (Fig. 3). The PCA applied to the parietotemporal configuration showed that the greatest shape variation in this region was associated with the width of the middle part of the cranium, the position of the temporal lines, and the relative length of the mastoid processes (Fig. 4). The greatest variation in the shape of

the occipital bone was observed in the position of inion, i.e., the external occipital protuberance (Fig. 5).

Discrimination ability of size and shape

The CS of the neurocranium classified correctly 85.5% of crania. Concerning the separate neurocranial regions, the highest overall accuracy was achieved by the parietotemporal region, followed closely by the frontal bone. Compared to the former two regions, the CS of the occipital bone configuration classified the crania of both sexes with much lower accuracy (Table 3).

The classification accuracy achieved by the shape variables of the neurocranium was quite low showing values of less than 65% in males and females (Table 4). Among the separate neurocranial regions, the shape of the frontal bone yielded the highest accuracy result of 71.8%, followed by the occipital bone (70.2%) and the parietotemporal region, which achieved rather lower accuracy of 62.2%. The combination of shape variables and CS improved the classification results in all landmark configurations (Table 5). The greatest increase in accuracy after the inclusion of CS was observed for the whole configuration of the neurocranium and amounted to 28.9%, while the accuracy of the occipital bone increased by only 6%.

The results produced by the k-means clustering showed that the correct sex classification based on the shape variables was quite low in all configurations (53–59%). The

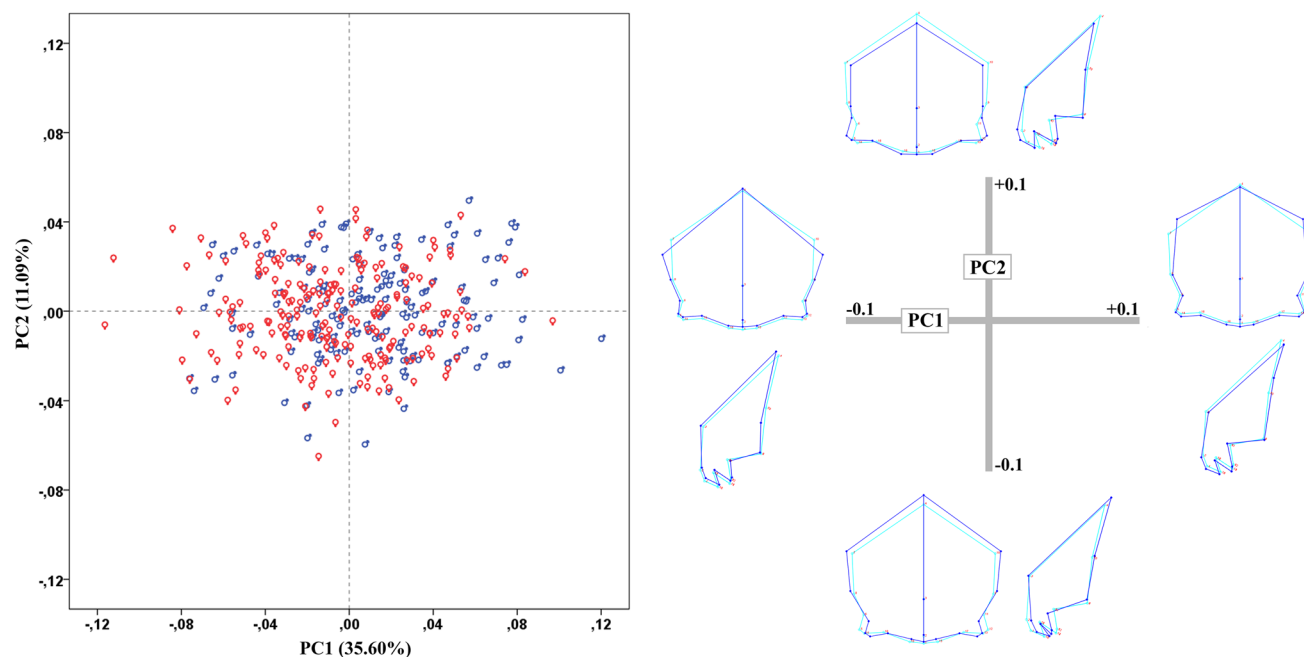


Fig. 3 Scatterplot of PC1 vs PC2 for the frontal bone. The wireframes illustrate the shape variation along the PC1 and PC2 axes. Blue male sign (♂) – male crania; red female sign (♀) – female crania

nia; light blue wireframe – the mean shape; dark blue wireframe – extreme shape configurations

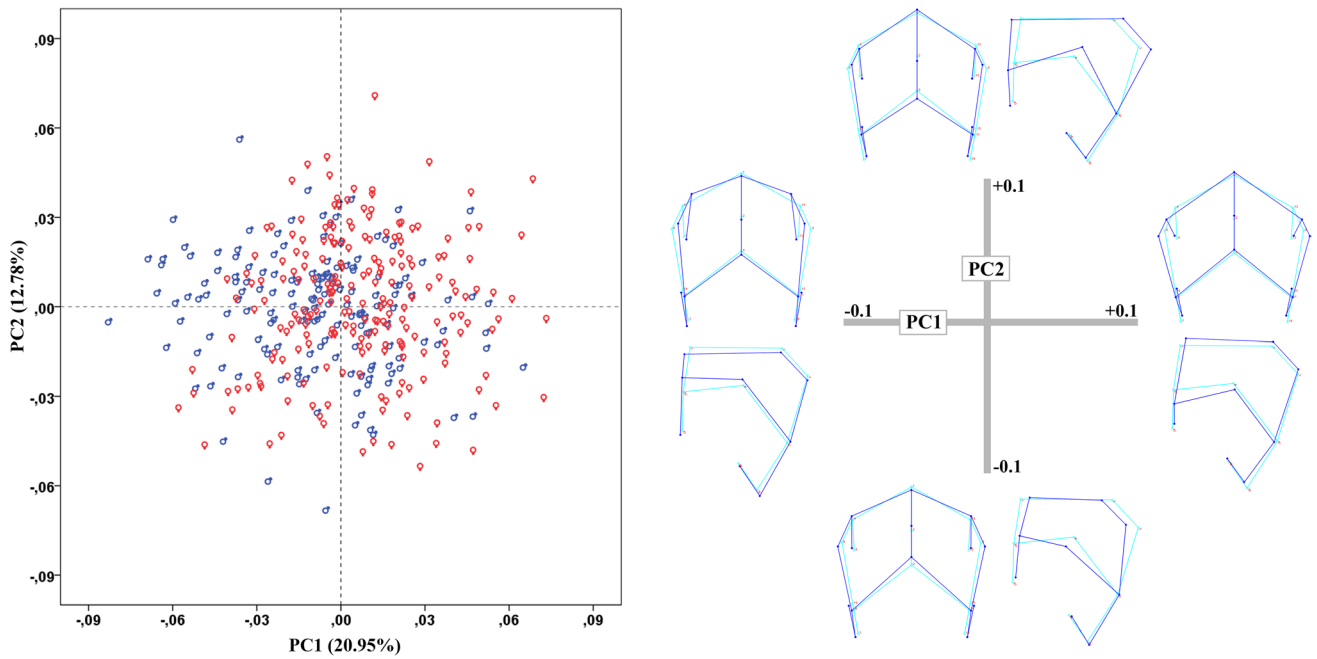


Fig. 4 Scatterplot of PC1 vs PC2 for the parietotemporal region. The wireframes illustrate the shape variation along the PC1 and PC2 axes. Blue male sign (♂) – male crania; red female sign (♀) – female crania

nia; light blue wireframe – the mean shape; dark blue wireframe – extreme shape configurations

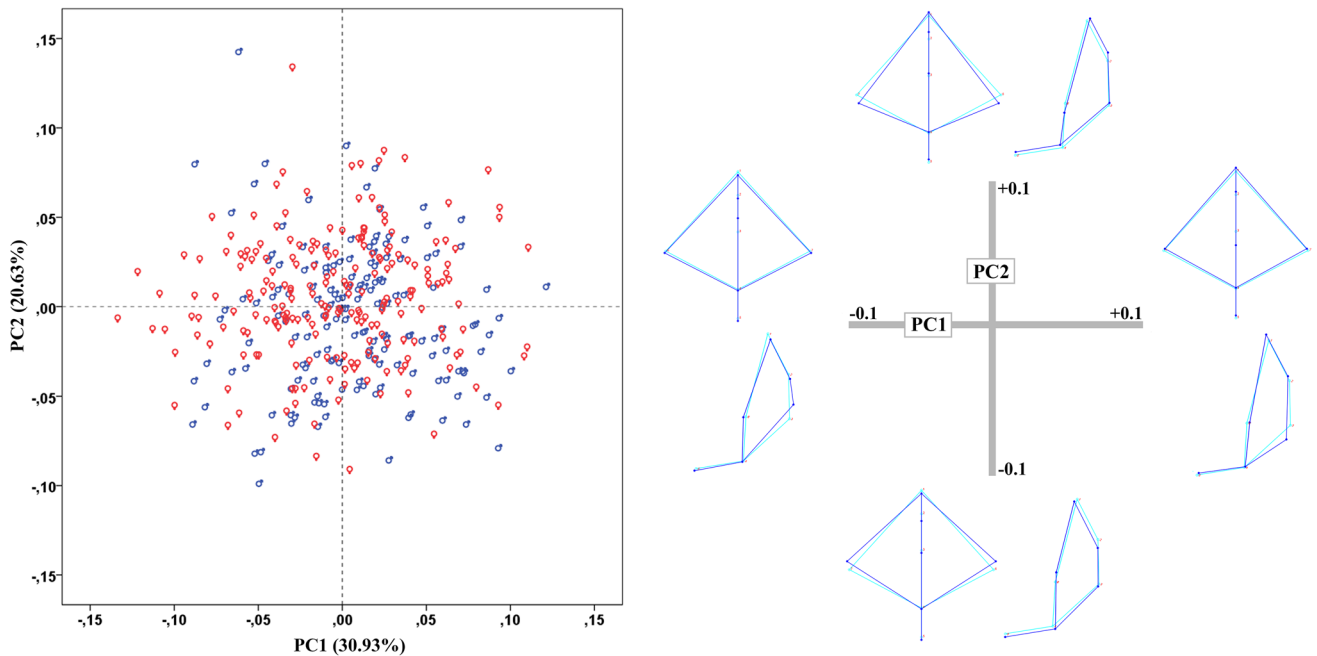


Fig. 5 Scatterplot of PC1 vs PC2 for the occipital bone. The wireframes illustrate the shape variation along the PC1 and PC2 axes. Blue male sign (♂) – male crania; red female sign (♀) – female crania

nia; light blue wireframe – the mean shape; dark blue wireframe – extreme shape configurations

male crania were classified with higher accuracy in all configurations, except for that of the whole neurocranium (Table 6). The classification results in the size-shape space

demonstrated a considerable increase in accuracy (up to 31.6% for the neurocranium configuration), except for the occipital bone. In almost all configurations herein, the

Table 3 Classification accuracy of the centroid size of the landmark configurations (in %)

Landmark configuration	Males	Females	Total
Neurocranium	81.4	88.7	85.5
Frontal bone	78.3	82.5	80.7
Parietotemporal region	76.4	85.4	81.5
Occipital bone	63.4	70.8	67.6

Table 4 Classification accuracy of the shape variables of the landmark configurations (in %)

Landmark configuration	Males	Females	Total
Neurocranium	61.5	64.6	63.3
Frontal bone	70.2	73.1	71.8
Parietotemporal region	59.6	64.2	62.2
Occipital bone	68.3	71.7	70.2

Table 5 Classification accuracy of the combined shape and size data of the landmark configurations (in %)

Landmark configuration	Males	Females	Total
Neurocranium	92.5	91.5	92.2
Frontal bone	83.9	89.2	86.9
Parietotemporal region	83.9	86.3	85.3
Occipital bone	74.5	77.4	76.1

Table 6 Results of the k-means cluster analysis

Landmark configuration	Shape			Shape + size		
	Males	Females	Total	Males	Females	Total
Neurocranium	53.4	55.7	54.7	79.5	91.5	86.3
Frontal bone	59.0	57.5	58.2	72.7	76.9	75.1
Parietotemporal region	63.4	55.2	58.7	70.8	92.0	82.8
Occipital bone	61.5	50.9	55.5	58.4	50.5	53.9

female crania were classified with higher accuracy compared to the male ones.

An additional configuration of the neurocranium, which included a reduced number of landmarks, was constructed to test its classification accuracy. The configuration consisted of 11 landmarks (nasion, glabella, metopion, opisthion, inion, right and left eurion, right and left stephanion, right and left mastoidale) depicting the anatomical loci of the neurocranium, which were most discernible between the male and female crania. It achieved accuracy of 84.7% (males: 80.1%; females: 88.2%) for the CS, 61.7% (males: 61.5%; females: 61.8%) for the shape variables, and 90.1% (males: 88.2%; females: 91.5%) for the combined data of shape and size. The results of the k-means clustering based on the

shape variables were considerably lower (50.9% for males and 54.2% for females) than those based on the combined shape and size variables (78.9% for males and 88.7% for females).

Discussion

The male and female crania in the present study differ significantly in the size of the neurocranium and its separate parts: frontal, middle (parietotemporal), and occipital. Significant sex differences in the CS of the cranium have been previously established [27, 28, 30, 36, 37]. Gonzalez et al. [38] have found that the male and female crania differ more in size than in shape. The size of the neurocranium has also been established to be a better sex discriminator than shape [39]. In our study, the size also outperforms the shape in all studied configurations, except for the occipital bone, where the shape classifies the male and female crania with slightly higher accuracy, though the accuracy results for this bone are very low. However, it should be taken into account that relying only on the size can lead to erroneous assessment of sex in some cases [40].

The traditional cranial measurements provide sex classification accuracy in the range 80–90% [10, 14, 41–44]. The discriminating ability of the CS in our study falls in the same range, except for the occipital bone. The highest accuracy is achieved by the CS of the whole configuration of the neurocranium. Similar accuracy results are achieved

by the CS of parietotemporal region and frontal bone. In all landmark configurations, the CS classifies more correctly the female crania, which has been previously observed as well [29, 30]. Although the CS of the occipital bone configuration shows significant sex differences, it fails in classifying sex correctly. Thus, the size of the frontal and middle part of the neurocranium appears to be more useful for sex estimation than that of the occipital bone.

Sexual dimorphism in cranial size is determined by genetic and environment factors. Normally, cranial size in males and females overlaps considerably up to 9 years of age, which indicates a low level of sexual dimorphism prior to the onset of puberty and/or the adolescent growth spurt

[45]. However, it has been suggested that sexual dimorphism in the size of neurocranium is predetermined in the prenatal period [46]. Yet, the development of the neurocranium to adult dimensions is influenced by epigenetic factors of high variability among populations, socioeconomic strata, geographical regions, etc. [47]. Thus, cranial dimensions reflect the effects of nutritional and environmental stress during growth [48]. Besides, males vary in cranial size in greater degree than females, which could be related to the longer time for completing cranial ontogeny as well as the plasticity and condition dependence of size [49]. All this shows that although predetermined to some extent, sexual dimorphism in the cranial size largely depends on the social and economic conditions in which the individuals of a given population grow up, which inevitably reflects on the discrimination potential of the developed size-based sexing methods for the population.

The shape of the neurocranium and its parts demonstrates significant sexual dimorphism in our study. Significant sex differences in the cranial shape have been established by other authors as well [36, 38]. However, Bigoni et al. [3] have not found such differences in the configuration of the neurocranium, except for the shape of its midsagittal curve. Morita et al. [50] have also reported low degrees of sexual dimorphism in cranial shape. Considering the F-statistics of PERMANOVA performed in our study, the frontal bone is the most sexually dimorphic neurocranial region in shape, while the parietotemporal region is the least differing one. Although all studied configurations demonstrate significant sex differences, the classification ability of their shape is very low with the best values slightly surpassing 70%. Among the separate neurocranial regions, the frontal bone provides the highest classification accuracy, followed by the occipital bone and the parietotemporal region. The classification accuracy provided by the whole configuration of the neurocranium is slightly higher than that of the parietotemporal region. The shape variables of all studied configurations classify the female crania with higher accuracy, which contradicts to the results of previous studies, where males have been classified more accurately than females [29, 37].

The shape analysis in previous studies has showed that male crania are more elongated in anteroposterior direction and the cranial vault in females tends to be more rounded and globular [3, 40, 51]. However, Green and Curnoe [28] have detected quite the opposite depiction where the male crania in lateral view are characterized with a more rounded vault contour, while the females are characterized by a more elongated cranial vault shape. There are also some contradictions concerning the cranial height. Lestrel et al. [40] have observed that the female crania are higher, but Chovalopoulou et al. [29] have reported that the cranial height is relatively invariable between the two sexes. Morphological differences between the male and female crania have

been previously established in the shape of the frontal bone curvature, glabellar region, mastoid processes, etc. The sex dissimilarities in these traits are considered manifestations of differences in the secondary sexual development [52], since no discernible pattern in the shape of the male and female crania has been registered in the prepubertal period [2, 53]. In our study, however, the PCA plot for the whole neurocranium does not show any clear separation of the male and female crania along the PC1 and PC2 axes associated namely with the abovementioned shape differences.

The separate neurocranial regions have been found to differ in the manifestation and strength of the sex differences. Nikita [36] have established that the anterior part of the cranium is more dimorphic than its posterior region. Similarly, by assessment of the lateral skull contour, Inoue et al. [54] established that the forehead shows significant sex differences, whereas such dissimilarities are not observed at the back of the head. Furthermore, the perception of a human head as masculine or feminine has been mostly related to sexually dimorphic traits located in the upper third of the face, such as the glabellar prominence, frontal eminences, and frontal inclination, i.e., in the frontal bone [55]. Hence, there are many arguments indicating that the shape of frontal bone is clearly discernible in adult males and females. It is well established that the male frontal bone is more inclined and has more prominent glabellar area compared to the female one [3, 28, 30, 37, 51, 52, 56–58]. The more rounded forehead in females [3] is related to a more superiorly positioned bregma along with a more anterior-inferiorly positioned midfrontal landmarks [37]. Besides, the lateral parts of the frontal bone along the coronal suture have also been reported as very dimorphic regions [18]. This refers mainly to the location of the landmark stephanion, which is relatively more superiorly located in males [50], while in female crania, the temporal lines are shorter in the vertical direction and their intersection with the coronal suture is positioned lower and anteriorly [58]. Moreover, the females have relatively wider transversal frontal bone dimensions [37], while the temporal lines in males are closer to the midsagittal plane [58]. Our observations on the frontal bone show the presence of significant sex differences in its shape, but the shape variation analysis demonstrates considerable overlapping between the males and females in our sample. Among the separate cranial regions studied herein, the frontal bone shape yields the best accuracy, though only 72%. This result is rather lower than those obtained in the previous studies, where the classification accuracy based on the shape of this bone have varied from 79 to 85% [18, 37, 58, 59]. However, it is worth noting that all these studies have applied PCA to the shape variables without controlling for the effect of size on shape, i.e., the allometry. Maass and Friedling [37] have observed higher accuracy when only the landmark configuration of frontal bone is used in comparison to the entire

neurocranium, which may be due to the fact that many of the sex-discriminating features are localized on this bone. Such a result is observed in our study as well, which comes to show that sexually dimorphic structures of the frontal bone contribute substantially to the correct sex classification.

In the present study, the shape of the middle part of the neurocranium provides the lowest classification accuracy compared to the other neurocranial parts. The parietal bones are rarely used in methods for sex estimation. According to Chovalopoulou et al. [29], the parietal region in males is wider than that in females. However, Green and Curnoe [28] and Maass and Friedling [52] have observed that the female crania are characterized by a relatively wider parietal region of the cranial vault. The mastoid process is the most exploited anatomical structure of the temporal bone for sex estimation. Various studies have established that the male mastoid processes are more robust and inferiorly projected than the female ones [60]. The ontogenetic changes in the projection of the mastoid process are related to biomechanical and functional loading of the bone, since the development and use of sternocleidomastoid muscle induce growth in its site of insertion, i.e., the mastoid process [2]. Since the biomechanical loading differs in males and females, this reflects on the sex differences in mastoid shape and size.

The occipital bone, more specially the nuchal region, is a frequently used feature in sex estimation, since it is more prominent and robust in males due to the muscle attachments [51]. However, the nuchal crest has been found to be a weak sex dimorphic trait [61]. The previous observations on the shape differences between the male and female occipital bones have indicated the following peculiarities: more superiorly and posteriorly positioned inion in female crania [28] in contrast to the more downward projection of inion in male crania [26]; more superiorly and anteriorly positioned lambda in male crania [26]; relatively longer occipital region in antero-posterior direction in female crania [52]; and more laterally positioned landmarks asterion in female crania [28]. Our results show that the occipital bone configuration is the second dimorphic part of the cranium after the frontal bone, but the classification accuracy is rather low (70%). Moreover, our PCA results do not show any visible separation of the male and female occipital bones along the axes of the first PCs. Generally, the large overlapping between the males and females on the PCA plots of all configurations demonstrates that the variance captured by the first two PCs could not be explained by sex-related variation in cranial morphology.

Both the size and shape are important components of sexual dimorphism that is why it has been suggested to consider them together in sex estimation process [28]. It has been established that the addition of CS to the shape data considerably increases the classification accuracy [10, 18, 27, 30, 38, 62]. It is common that the inclusion of CS provides

classification accuracy of around and more than 90% [39, 51, 62]. Thus, the shape and size together produce better accuracy results than using the size only [39]. Moreover, the combined data of CS and shape variables have outperformed the accuracy results based on shape variables only by approximately 10% for both males and females [28, 29] and even more than 15% in total [38]. However, Musilova et al. [51] have not reported such big differences between the results in the form and shape space (with an overall difference of 3%). In our study, the combination of CS and shape variables leads to considerable increase (up to 29%) in accuracy, which does show an enormous contribution of the CS to the sex estimation. Yet, in the configurations of the occipital bone, it yields a gain in accuracy of only 6%. The results of the k-means cluster analysis also demonstrate a significant increase in the correct classification after the addition of size (up to 32% for the configuration of the whole neurocranium). This indicates that combined shape and size data provide a good basis for correct clustering of the male and female crania without initial information about their sex but only based on their morphological similarity. Besides, the high result obtained for the female crania in the size-shape space indicates that the morphological resemblance in females is larger than that in males.

The accuracy results achieved by the whole configuration of the neurocranium in our study are based on a set of 32 landmarks. However, if we use only 11 landmarks appointing the most discernible anatomical structures of the neurocranium, the obtained results are also higher than those based on the frontal bone, parietotemporal region, and occipital bone. The only exception is the accuracy obtained in the shape space, where all other configurations perform better than the reduced landmark set of the neurocranium. The accuracy of nearly 90% achieved on the combined data of shape and CS demonstrates further the strong classification ability of the reduced landmark set in the size-shape space. This indicates that namely the landmarks included in the reduced dataset contribute most substantially to the discrimination between the male and female neurocranium. Thus, our results confirm the statement of Maass and Friedling [37] that a small number of landmarks could be sufficient for correct discrimination between the male and female crania.

Conclusion

The neurocranium in males and females differs significantly in its shape and size. In the target population, the size of the neurocranium is a better sex indicator than its shape, but the classification accuracy is increased when the shape and size data are analyzed together. The size-related sex differences are mainly observed in the parietotemporal region and

frontal bone. The most pronounced sex differences in shape are focused on the frontal bone, although the sex discrimination ability based on the shape variables is generally low in all configurations. When the combined shape and size data are used for sex classification, the discrimination ability decreases in anteroposterior direction from the frontal bone to the occipital region. Therefore, size contributes more significantly to the sex differences between male and female neurocrania than shape, and accordingly, the frontal and middle parts of the neurocranium are more reliable sources of data for sex estimation than its posterior part.

Supplementary Information The online version contains supplementary material available at <https://doi.org/10.1007/s00414-022-02876-0>.

Author contribution Diana H. Toneva: conceptualization, methodology, formal analysis, investigation, validation, data curation, visualization, writing—original draft. Silviya Y. Nikolova: conceptualization, methodology, investigation, writing—review and editing, project administration, funding acquisition. Elena D. Tasheva-Terzieva: formal analysis, methodology, data curation, writing—review and editing. Dora K. Zlatareva: resources, writing—review and editing. Nikolai E. Lazarov: writing—review and editing.

Funding This study was funded by the Bulgarian National Science Fund (Grant number KII-06-H51/4 – 11.11.2021).

Declarations

Ethics approval This study was performed in line with the principles of the Declaration of Helsinki. Approval was granted by the Human Research Ethics Committee at the Institute of Experimental Morphology, Pathology and Anthropology with Museum, Bulgarian Academy of Sciences (No. 12/29.10.2021).

Conflict of interest The authors declare no competing interests.

References

- Scheuer L (2002) Application of osteology to forensic medicine. *Clin Anat* 15:297–312
- Noble JME (2015) Morphometrics of the juvenile skull analysis of ontogenetic growth patterns. MA Thesis, University of Western Australia, Perth
- Bigoni L, Velemínská J, Bružek J (2010) Three-dimensional geometric morpho-metric analysis of cranio-facial sexual dimorphism in a Central European sample of known sex. *Homo* 61:16–32. <https://doi.org/10.1016/j.jchb.2009.09.004>
- Bewes J, Low A, Morphett A, Pate F, Henneberg M (2019) Artificial intelligence for sex determination of skeletal remains: application of a deep learning artificial neural network to human skulls. *J Forensic Legal Med* 62:40–43. <https://doi.org/10.1016/j.jflm.2019.01.004>
- Yang W, Liu X, Wang K, Hu J, Geng G, Feng J (2019) Sex determination of three-dimensional skull based on improved backpropagation neural network. *Comput Math Methods Med* 2019:9163547–9163548. <https://doi.org/10.1155/2019/9163547>
- Toneva DH, Nikolova SY, Agre GP, Zlatareva DK, Hadjidekov VG, Lazarov NE (2020) Data mining for sex estimation based on cranial measurements. *Forensic Sci Int* 315:110441. <https://doi.org/10.1016/j.forsciint.2020.110441>
- Bertsatos A, Chovalopoulou ME, Brůžek J, Bejdová Š (2020) Advanced procedures for skull sex estimation using sexually dimorphic morphometric features. *Int J Legal Med* 134:1927–1937. <https://doi.org/10.1007/s00414-020-02334-9>
- Toneva D, Nikolova S, Agre G, Zlatareva D, Hadjidekov V, Lazarov N (2021) Machine learning approaches for sex estimation using cranial measurements. *Int J Legal Med* 135:951–966. <https://doi.org/10.1007/s00414-020-02460-4>
- Shearer BM, Sholts SB, Garvin HM, Wärmklärer SK (2012) Sexual dimorphism in human browridge volume measured from 3D models of dry crania: a new digital morphometrics approach. *Forensic Sci Int* 222:400.e1–5. <https://doi.org/10.1016/j.forsciint.2012.06.013>
- Franklin D, Cardini A, Flavel A, Kuliukas A (2012) The application of traditional and geometric morphometric analyses for forensic quantification of sexual dimorphism: preliminary investigations in a Western Australian population. *Int J Leg Med* 126:549–558. <https://doi.org/10.1007/s00414-012-0684-8>
- Franklin D, Cardini A, Flavel A, Kuliukas A (2013) Estimation of sex from cranial measurements in a Western Australian population. *Forensic Sci Int* 229:158e1–158e8. <https://doi.org/10.1016/j.forsciint.2013.03.00>
- Dillon A (2014) Cranial sexual dimorphism and the population specificity of anthropological standards. Master Thesis, University of Western Australia, p 106
- Ekizoglu O, Hocaoglu E, Inci E, Can IO, Solmaz D, Aksoy S, Buran CF, Sayin I (2016) Assessment of sex in a modern Turkish population using cranial anthropometric parameters. *Legal Med* 21:45–52. <https://doi.org/10.1016/j.legalmed.2016.06.001>
- Ibrahim A, Alias A, Nor FM, Swarhib M, Bakar AN, Das S (2017) Study of sexual dimorphism of Malaysian crania: an important step in identification of the skeletal remains. *Anat Cell Biol* 50:86–92. <https://doi.org/10.5115/acb.2017.50.2.86>
- Zaafrane M, Ben KM, Naccache I, Ezzedine E, Savall F, Telmon N, Mnif N, Hamdoun M (2017) Sex determination of a Tunisian population by CT scan analysis of the skull. *Int J Legal Med* 132:853–862. <https://doi.org/10.1007/s00414-017-1688-1>
- Bejdová Š, Dupej J, Krajiček V, Velemínská J, Velemínský P (2018) Stability of upper face sexual dimorphism in central European populations (Czech Republic) during the modern age. *Int J Legal Med* 132:321–330. <https://doi.org/10.1007/s00414-017-1625-3>
- Gao H, Geng G, Yang W (2018) Sex determination of 3D skull based on a novel unsupervised learning method. *Comput Math Methods Med* 2018:4567267. <https://doi.org/10.1155/2018/456726>
- Cechová M, Dupej J, Bružek J, Bejdová Š, Horák M, Velemínská J (2019) Sex estimation using external morphology of the frontal bone and frontal sinuses in a contemporary Czech population. *Int J Legal Med* 133:1285–1294. <https://doi.org/10.1007/s00414-019-02063-8>
- Yang W, Zhou M, Zhang P, Geng G, Liu X, Zhang H (2020) Skull sex estimation based on wavelet transform and Fourier transform. *Biomed Res Int* 2020:8608209–8608210. <https://doi.org/10.1155/2020/8608209>
- Ramsthaler F, Kettner M, Gehl A, Verhoff MA (2010) Digital forensic osteology: morphological sexing of skeletal remains using volume-rendered cranial CT scans. *Forensic Sci Int* 195:148–152. <https://doi.org/10.1016/j.forsciint.2009.12.010>
- Franklin D, Freedman L, Milne N (2005) Sexual dimorphism and discriminant function sexing in indigenous South African crania. *Homo* 55:213–228

22. Pérez-Claros JA, Jiménez-Arenas JM, Palmqvist P (2015) Neurocranium versus face: a morphometric approach with classical anthropometric variables for characterizing patterns of cranial integration in extant hominoids and extinct hominins. *PLoS One* 10(7):e0131055. <https://doi.org/10.1371/journal.pone.0131055>
23. Bastir M, Rosas A, O'Higgins P (2006) Craniofacial levels and the morphological maturation of the human skull. *J Anat* 209:637–654. <https://doi.org/10.1111/j.1469-7580.2006.00644.x>
24. Cabo L, Brewster C, Azpiazu JL (2012) Sexual dimorphism: interpreting sex markers. In: Dirkmaat D (ed) *A companion to forensic anthropology*. John Wiley & Sons Ltd, Chichester, pp 248–286
25. Weisensee KE, Jantz RL (2011) Secular changes in craniofacial morphology of the Portuguese using geometric morphometrics. *Am J Phys Anthropol* 145:548–559. <https://doi.org/10.1002/ajpa.21531>
26. Rosas A, Bastir M (2002) Thin-plate spline analysis of allometry and sexual dimorphism in the human craniofacial complex. *Am J Phys Anthropol* 117:236–245. <https://doi.org/10.1002/ajpa.10023>
27. Kimmerle EH, Ross A, Slice DE (2008) Sexual dimorphism in America: geometric morphometric analysis of the craniofacial region. *J Forensic Sci* 53:54–57
28. Green H, Curnoe D (2009) Sexual dimorphism in Southeast Asian crania: a geometric morphometric approach. *Homo* 60:517–534. <https://doi.org/10.1016/j.jchb.2009.09.001>
29. Chovalopoulou ME, Valakos ED, Manolis SK (2016) Sex determination by three-dimensional geometric morphometrics of the vault and midsagittal curve of the neurocranium in a modern Greek population sample. *Homo* 67:173–187. <https://doi.org/10.1016/j.jchb.2015.09.007>
30. Best KC, Garvin HM, Cabo LL (2017) An investigation into the relationship between human cranial and pelvic sexual dimorphism. *J Forensic Sci* 63:990–1000. <https://doi.org/10.1111/1556-4029.13669>
31. Cignoni P, Callieri M, Corsini M, Dellepiane M, Ganovelli F, Ranzuglia G (2008) MeshLab: an open-source mesh processing tool. In: Scarano V, de Chiara R, Erra U (eds) *Sixth eurographics Italian chapter conference*. Eurographics Association, Salerno, pp 129–136
32. Klingenberg CP (2011) MorphoJ: an integrated software package for geometric morphometrics. *Mol Ecol Resour* 11(2):353–357. <https://doi.org/10.1111/j.1755-0998.2010.02924.x>
33. Hammer Ø, Harper DAT, Ryan PD (2001) PAST: paleontological statistics software package for education and data analysis. *Palaeontol Electron* 4:9–18
34. Zhang Z, Yuan K-H (2018) *Practical statistical power analysis using Webpower and R* (Eds). ISDSA Press, Granger, IN. <https://webpower.psychstat.org/models/kurtosis/>. Accessed Nov 2021
35. Koo TK, Li MY (2016) A guideline of selecting and reporting intraclass correlation coefficients for reliability research. *J Chiropr Med* 15:155–163. <https://doi.org/10.1016/j.jcm.2016.02.012>
36. Nikita E (2012) Age-associated variation and sexual dimorphism in adult cranial morphology: implications in anthropological studies. *Int J Osteoarchaeol* 24:557–569. <https://doi.org/10.1002/oa.2241>
37. Maass P, Friedling LJ (2020) Morphometric variation of the frontal bone in an adult South African cadaveric sample. *Homo* 71:205–218. <https://doi.org/10.1127/homo/2020/1120>
38. Gonzalez PN, Bernal V, Perez SI (2011) Analysis of sexual dimorphism of craniofacial traits using geometric morphometric techniques. *Int J Osteoarchaeol* 21:82–91. <https://doi.org/10.1002/oa.1109>
39. Chovalopoulou ME, Bertsatos A (2018) Exploring the shape variation of the human cranium. A geometric morphometrics study on a modern Greek population sample. In: Rissech C, Lloveras L, Nadal J, Fullola JM (eds) *Geometric morphometrics*. Trends in biology, paleobiology and archaeology. SERP-UB, Barcelona, pp 25–39
40. Lestrel PE, Kanazawa E, Wolfe CA (2011) Sexual dimorphism using elliptical Fourier analysis: shape differences in the craniofacial complex. *Anthropol Sci* 119:213–229
41. Giles E, Elliot O (1963) Sex determination by discriminant function analysis of crania. *Am J Phys Anthropol* 21:53–68
42. Steyn M, Iscan MY (1998) Sexual dimorphism in the crania and mandibles of South African whites. *Forensic Sci Int* 98:9–16. [https://doi.org/10.1016/s0379-0738\(98\)00120-0](https://doi.org/10.1016/s0379-0738(98)00120-0)
43. Dayal MR, Spocter MA, Bidmos MA (2008) An assessment of sex using the skull of black south Africans by discriminant function analysis. *Homo* 59:209–221. <https://doi.org/10.1016/j.jchb.2007.01.001>
44. Ogawa Y, Imaizumi K, Miyasaka S, Yoshino M (2013) Discriminant functions for sex estimation of modern Japanese skulls. *J Forensic Legal Med* 20:234–238. <https://doi.org/10.1016/j.jflm.2012.09.023>
45. Noble J, Cardini A, Flavel A, Franklin D (2019) Geometric morphometrics on juvenile crania: exploring age and sex variation in an Australian population. *Forensic Sci Int* 294:57–68. <https://doi.org/10.1016/j.forsciint.2018.10.022>
46. Bulygina E, Mitteroecker P, Aiello L (2006) Ontogeny of facial dimorphism and patterns of individual development within one human population. *Am J Phys Anthropol* 131:432–443
47. Zavando MDA, Suazo GIC, Smith RL (2009) Sexual dimorphism determination from the lineal dimensions of skulls. *Int J Morphol* 27:133–137
48. Angel JL (1982) A new measure of growth efficiency: skull base height. *Am J Phys Anthropol* 58:297–305
49. Milella M, Franklin D, Belcastro MG, Cardini A (2021) Sexual differences in human cranial morphology: is one sex more variable or one region more dimorphic? *Anat Rec (Hoboken)* 304:2789–2810. <https://doi.org/10.1002/ar.24626>
50. Morita Y, Ogiwara N, Kanai T, Suzuki H (2013) Technical note: quantification of neurocranial shape variation using the shortest paths connecting pairs of anatomical landmarks. *Am J Phys Anthropol* 151:658–666. <https://doi.org/10.1002/ajpa.22315>
51. Musilová B, Dupej J, Veleřinská J, Chaumoitre K, Bruzek J (2016) Exocranial surfaces for sex assessment of the human cranium. *Forensic Sci Int* 269:70–77
52. Maass P, Friedling LJ (2019) Morphometric analysis of the neurocranium in an adult South African cadaveric sample. *J Forensic Sci* 64:367–374. <https://doi.org/10.1111/1556-4029.13878>
53. Garcovich D, Albert Gasco L, Alvarado Lorenzo A, Aiuto R, Adobes Martin M (2022) Sex estimation through geometric morphometric analysis of the frontal bone: an assessment in pre-pubertal and post-pubertal modern Spanish population. *Int J Legal Med* 136:319–328. <https://doi.org/10.1007/s00414-021-02712-x>
54. Inoue M, Inoue T, Fushimi Y, Okada K (1992) Sex determination by discriminant function analysis of lateral cranial form. *Forensic Sci Int* 57:109–117. [https://doi.org/10.1016/0379-0738\(92\)90003-f](https://doi.org/10.1016/0379-0738(92)90003-f)
55. Petaros A, Garvin HM, Sholts SB, Schlager S, Wärländer SKTS (2017) Sexual dimorphism and regional variation in human frontal bone inclination measured via digital 3D models. *Leg Med (Tokyo)* 29:53–61. <https://doi.org/10.1016/j.legalmed.2017.10.001>
56. Franklin D, Freedman L, Milne N, Oxnard CE (2007) Geometric morphometric study of population variation in indigenous southern African crania. *Am J Hum Biol* 19:20–33. <https://doi.org/10.1002/ajhb.20569>
57. Murphy RE, Garvin HM (2018) A morphometric outline analysis of ancestry and sex differences in cranial shape. *J Forensic Sci* 63:1001–1009. <https://doi.org/10.1111/1556-4029.13699>

58. del Bove A, Profico A, Riga A, Bucchi A, Lorenzo C (2020) A geometric morphometric approach to the study of sexual dimorphism in the modern human frontal bone. *Am J Phys Anthropol* 173:643–654. <https://doi.org/10.1002/ajpa.24154>
59. Inoue M (1990) Fourier analysis of the forehead shape of skull and sex determination by use of computer. *Forensic Sci Int* 47:101–112. [https://doi.org/10.1016/0379-0738\(90\)90204-C](https://doi.org/10.1016/0379-0738(90)90204-C)
60. Jung H, Woo EJ (2016) Evaluation of mastoid process as sex indicator in modern White Americans using geometric morphometrics. *J Forensic Sci* 61:1029–1033. <https://doi.org/10.1111/1556-4029.13079>
61. Garvin HM, Sholts SB, Mosca LA (2014) Sexual dimorphism in human cranial trait scores: effects of population, age, and body size. *Am J Phys Anthropol* 154:259–269
62. Franklin D, O'Higgins P, Oxnard CE, Dadour I (2007) Sexual dimorphism and population variation in the adult mandible: forensic applications of geometric morphometrics. *Forensic Sci Med Pathol* 3:15–22. <https://doi.org/10.1385/FSMP:3:1:15>

Publisher's note Springer Nature remains neutral with regard to jurisdictional claims in published maps and institutional affiliations.

Springer Nature or its licensor holds exclusive rights to this article under a publishing agreement with the author(s) or other rightsholder(s); author self-archiving of the accepted manuscript version of this article is solely governed by the terms of such publishing agreement and applicable law.